

Design of a Muon Accelerator Driver for a Neutrino Factory

J. Delayen, D. Douglas, L. Harwood, G. Krafft, V. Lebedev, Ch. Leemann, and L. Merminga

Overview

The neutrino factory is to be driven by a high energy muon accelerator driver (MAD). This machine will capture 190 MeV muons from the source [1] and accelerate them to 50 GeV. Gross machine parameters are given in Table 1; Table 2 presents derived machine parameters (such as average and peak currents) that will be of use in subsequent discussions.

Table 1: System Parameters

Parameter	Baseline Value
$P_{\text{injection}}$	190 MeV/c
E_{final}	50 GeV
$\epsilon_N^{\text{injected}}$	1.5 mm-rad
$\epsilon_N^{\text{extracted}}$	3.2 mm-rad
$\Delta E/E_{\text{final}}$	$< \pm 2\%$
$\sigma_l^{\text{bunch, injected}}$	12 cm
$\sigma_{\delta p/p}^{\text{bunch, injected}}$	11%
macropulse length	four 150 nsec pulses with 250 nsec pulse-to-pulse separation
$N_{\text{bunch/macropulse}}$	$30 \times 4 = 120$
$N_{\mu/\text{macropulse, extracted}}$	3×10^{12}
$f_{\text{macropulse}}$	15 Hz

Table 2: Derived Parameters

Parameter	Derived Value	Comments
I_{ave}	7.2 μA	Macroscopic average current
$I_{\text{in pulse}}$	0.8 A	Current in quarter-macropulse
P_{ave}	360 kW	Macroscopic average beam power
$P_{\text{in pulse}}$	40 GW	Beam power in quarter-macropulse
$\beta_{\text{injection}} = v/c$	0.87	
$\epsilon_{\text{injected}}^{\text{geometric}} = \epsilon_N^{\text{injected}} / \beta\gamma$	9×10^{-4} m-rad	Injected geometric emittance
$\epsilon_{\text{extracted}}^{\text{geometric}} = \epsilon_N^{\text{extracted}} / \beta\gamma$	6.4×10^{-6} m-rad	Extracted geometric emittance
$\sigma_{\text{betatron}}^{\text{injected}} (\beta=1 \text{ m})$	3 cm	Injected rms spot size at beam envelope of 1 m
$\sigma_{\text{betatron}}^{\text{extracted}} (\beta=10 \text{ m})$	8 mm	Extracted rms spot size at beam envelope of 10 m

Fundamental Issues

The primary technical issues influencing the performance of this system are as follows:

- muon survival,
- choice of accelerating technology and frequency,
- accelerator acceptance – capture, acceleration, and transport of the large source muon phase space, and
- accelerator performance – issues such as potential collective effects (such as BBU) resulting from the relatively high beam current during the muon macropulse.

Muon Survival – As an unstable species, muons from the source will decay during the beam handling process. It is therefore critical to capture and accelerate the injected source beam as rapidly as possible. Figure 1 shows fractional muon survival as a function of distance along the machine at various RF real-estate gradients. It is apparent that average gradients in excess of 5 MV/m are adequate to ensure a significant fraction of the initial beam survives to be injected into the neutrino factory storage ring.

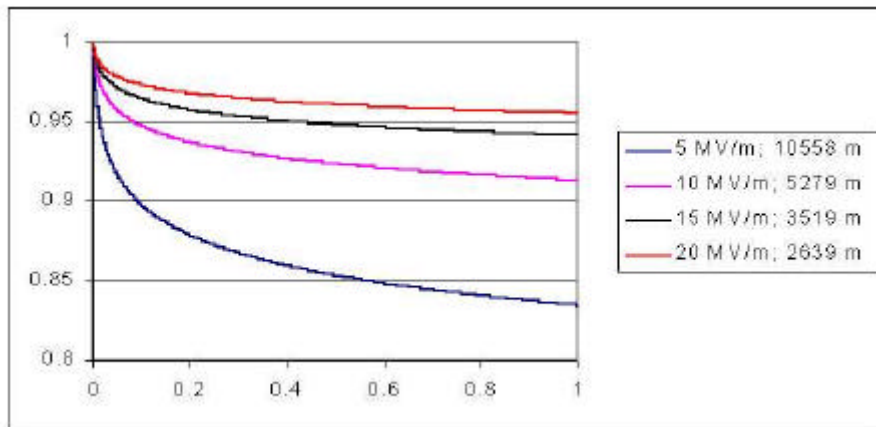


Figure 1: Muon survival for 0 to 50 GeV as a function of real-estate gradient and fractional distance along machine.

Selection of Acceleration Technology – Muon survival requirements demand the MAD be a linac; source requirements demand it be 200 MHz or a higher harmonic thereof. Beyond these rudimentary constraints, there are a number of available technologies, which can be summarized by selections from the following list:

- straight/recirculated linac
- conventional/SRF technology
- CW/pulsed RF
 - “fast” – on microsecond time scales, will fill times prompt with the beam pulse, or
 - “slow” – on millisecond time scales, filling cavities between beam pulses and accelerating beam macropulses using stored energy.

Wall losses and RF power demands prohibit the use of recirculation and “slow pulse” scenarios with copper linacs. Gradients achievable with CW conventional RF are too low for adequate muon survival. High instantaneous RF drive power demands ($0.8 \text{ A} \times 50 \text{ GeV} = 40 \text{ GW}$ in each quarter of the macropulse) with associated high costs eliminate “fast fill” pulsed conventional or SRF systems. The scenario of choice is therefore slow pulsed (slow fill at 15 Hz while beam is off/accelerate using stored energy) or CW SRF, with either straight or recirculated transport.

Recirculation provides cost savings over a single linac. The number of acceleration stages and passes per stage is a more detailed question. Jefferson Lab experience with recirculating linacs suggests that muon recirculation should be possible at energies in excess of 3 GeV. For the imposing initial emittance and energy spread it is found that a ratio of final to injected energy well below 10 to 1 is very desirable [2]. We therefore propose a machine architecture using a 0.2 to 3 GeV preaccelerator, a 3 to 10 GeV “compressor” recirculating linear accelerator (RLA1), and a 10 to 50 GeV “primary” recirculating linear accelerator (RLA2). The *preaccelerator* captures the large source phase space and accelerates it to relativistic energies. At this point, the longer lab frame muon lifetime allows the *compressor* (RLA1) to be used to manipulate the longitudinal and transverse phase spaces (while further raising the energy) for injection in to a high energy *primary* (RLA2). This accelerates the preaccelerator- and compressor-conditioned phase space to the 50 GeV injection energy of the neutrino factory storage ring.

Microbunch spacing from the muon source requires the RF frequency be 200 MHz or one of its harmonics. The frequency of choice for both preaccelerator and compressor is clearly 200 MHz, as it provides large physical apertures and adequate transverse and longitudinal acceptance for the large source beam. It also has adequate stored energy to accelerate multiple passes of a single pulse bunch train without RF overhead, allowing use of the “slow fill” pulsed scenario.

The choice is less obvious for RLA2, inasmuch as the phase space is smaller and rather more manageable. Preliminary studies suggest the second harmonic, 400 MHz, may provide adequate aperture and acceptance. This would as well provide significant cost savings over 200 MHz. Detailed calculations show that the availability of large stored energy at 200 MHz (contrasted to four times smaller at 400 MHz) and the long 200 MHz RF wavelength allows smaller beam momentum spread through the driver acceleration cycle, and will likely meet performance requirements. This is due to both better bunch length to wavelength ratio and relatively smaller gradient sag due to beam loading over the macropulse (due to the larger stored energy at 200 MHz). This alleviates transport acceptance demands in the driver recirculator. It is not clear however that this is necessary. The following “solution in progress” attempts to provide adequate recirculator acceptance to manage the larger momentum spread (and tighter bunch length tolerances) associated with 400 MHz. Preliminary results suggest it, too, will provide the required performance. Because of significant cost savings, it is therefore our choice of frequency for the primary. If, during ongoing design work it becomes apparent that 400 MHz will not provide adequate performance, the 200 MHz solution used in the preaccelerator and

compressor will meet requirements and can, without additional R&D, be implemented in RLA2 as well.

Machine Architecture

We proposed a MAD machine architecture based on a chain of three accelerators. A preaccelerator is used to bring the beam to relativistic energies, where recirculation can be invoked. A compressor (RLA1) is then used to condition the phase space by raising the beam energy and adiabatically damping geometric emittances, relative momentum spread and bunch length, so as to render the phase space volume manageable for a primary accelerator (RLA2). The principle beam dynamics issues are as follows:

- capture (longitudinal and transverse) of the large injected phase space,
- minimum recirculatable energy,
- acceleration/longitudinal matching scenarios in the compressor to condition the phase space for subsequent acceleration to full energy,
- design of RLA1 and 2, including initial and final energy, number of passes, and beamline optics providing adequate acceptance as well as support for the required longitudinal manipulations, and
- potential instabilities (such as BBU) at the relatively high ~ 1 A instantaneous currents present in the macropulse.

An “existence proof” design with sufficient (though perhaps better than necessary) performance to address these issues has evolved based on the above machine concept. As the large injected phase space is a primary concern, the design process first developed a longitudinal capture and acceleration scenario [3] which indicates a 200 MHz 3 GeV preaccelerator would provide adequate capture and high enough energy for recirculation and longitudinal matching in RLA1. A 3 to 10 GeV RLA1 concept based on a 4 pass, 200 MHz recirculator was then developed. The energy range and pass number were deemed prudently conservative, from a geometric and beam dynamics viewpoint, to accommodate the splitting, recirculation, and recombination of the large beam phase space on multiple passes, while providing adequate opportunity for longitudinal matching manipulations. Acceleration phases and momentum compactions were selected so as to provide compression of both relative momentum spread and bunch length. A similar process was followed for RLA2, which provides in 5 passes primary acceleration from 10 to 50 GeV. As noted above, preliminary results suggest a 400 MHz system will provide adequate RLA2 performance (though with larger intermediate momentum spreads than in a 200 MHz system). Figure 2 presents longitudinal phase space behavior through such a the system; required acceleration phases and momentum compactions are shown in Table 3. Simulations of the 400 MHz scenario are at present incomplete, but suggest the higher frequency will meet requirements. Should further study indicate performance is not adequate, a 200 MHz alternative has been studied in some detail [4]. This alternative does meet performance requirements and can be expected to be more operationally robust, though at a higher initial cost. For the purposes of this study, we will proceed with use of

400 MHz, inasmuch as it is likely to provide lower system and operating costs than 200 MHz, and will migrate to 200 MHz if it becomes a technical necessity.

Given a longitudinal scenario, a complete system solution was developed. The preaccelerator utilizes solenoid focussing between cryomodules. Beam envelopes are shown in Figure 3. The compressor, RLA1, comprises two 1.227 GeV linacs with multiple passes horizontally split and recombined using cascaded dipoles. Once separated, the individual beams are recirculated by periodic “bend-triplet-bend” arcs, typical beam envelope solutions for which are given in Figure 4. Chromatic behavior is adequate to accept 10% momentum spreads; sextupole correction of second order dispersion in spreaders and recombiners is necessary due to the broken periodicity. This is provided by a set of four sextupoles in the spreaders and recombiners and prevents growth of beam emittance. A similar approach was adopted for RLA2 (Figure 5). Cascaded dipoles split the five passes horizontally, bringing all parallel in a few tens of meters. As the linac is rather longer than in RLA1, additional matching capacity is provided following the beam separation; in each pass an array of quadrupoles provides matching of pass-to-pass linac beam envelopes to regular, horizontally separated FODO arcs. Again, as the focussing is modest and the structures regular, there is no anticipated requirement for chromatic correction beyond that expected in the spreader/recombiners. A machine footprint is presented in Figure 6. For clarity and ease of comparison, the various segments (preaccelerator, RLA1, and RLA2) are all positioned sequentially. In an actual construction design, economic prudence suggests a more compact layout, possibly with shared usage of tunnel and conventional facilities by multiple machine segments, be developed.

Figure 2a: Longitudinal phase space in RLA1

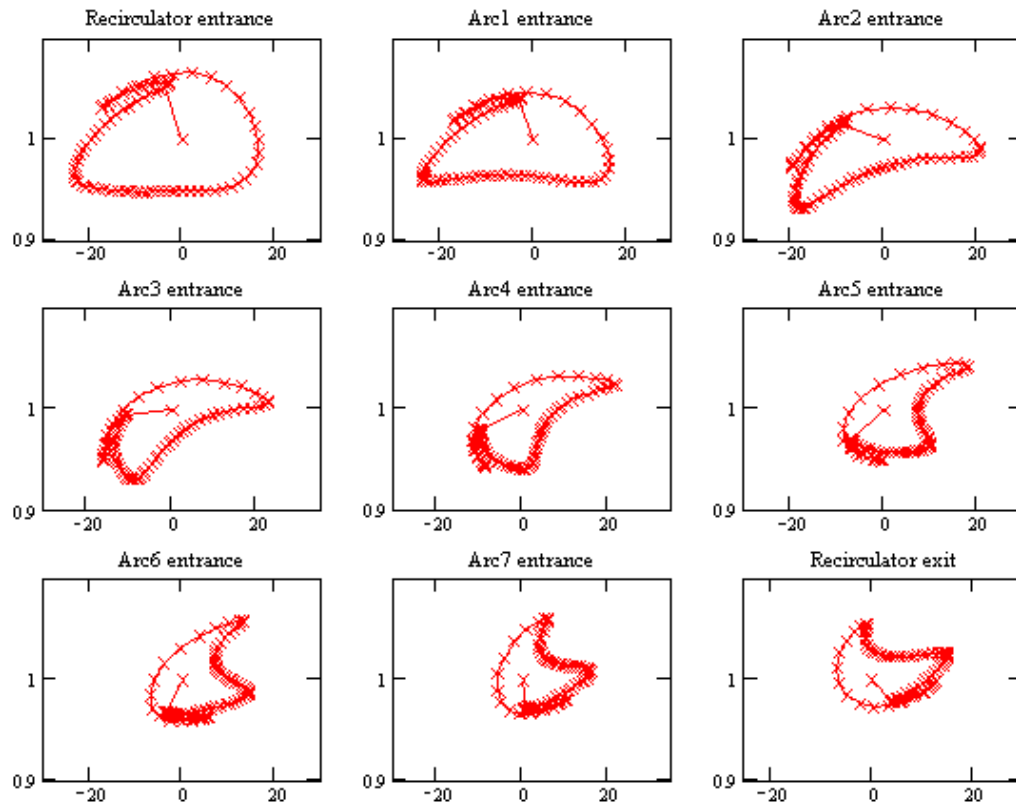


Figure 2b: Longitudinal phase space in RLA2

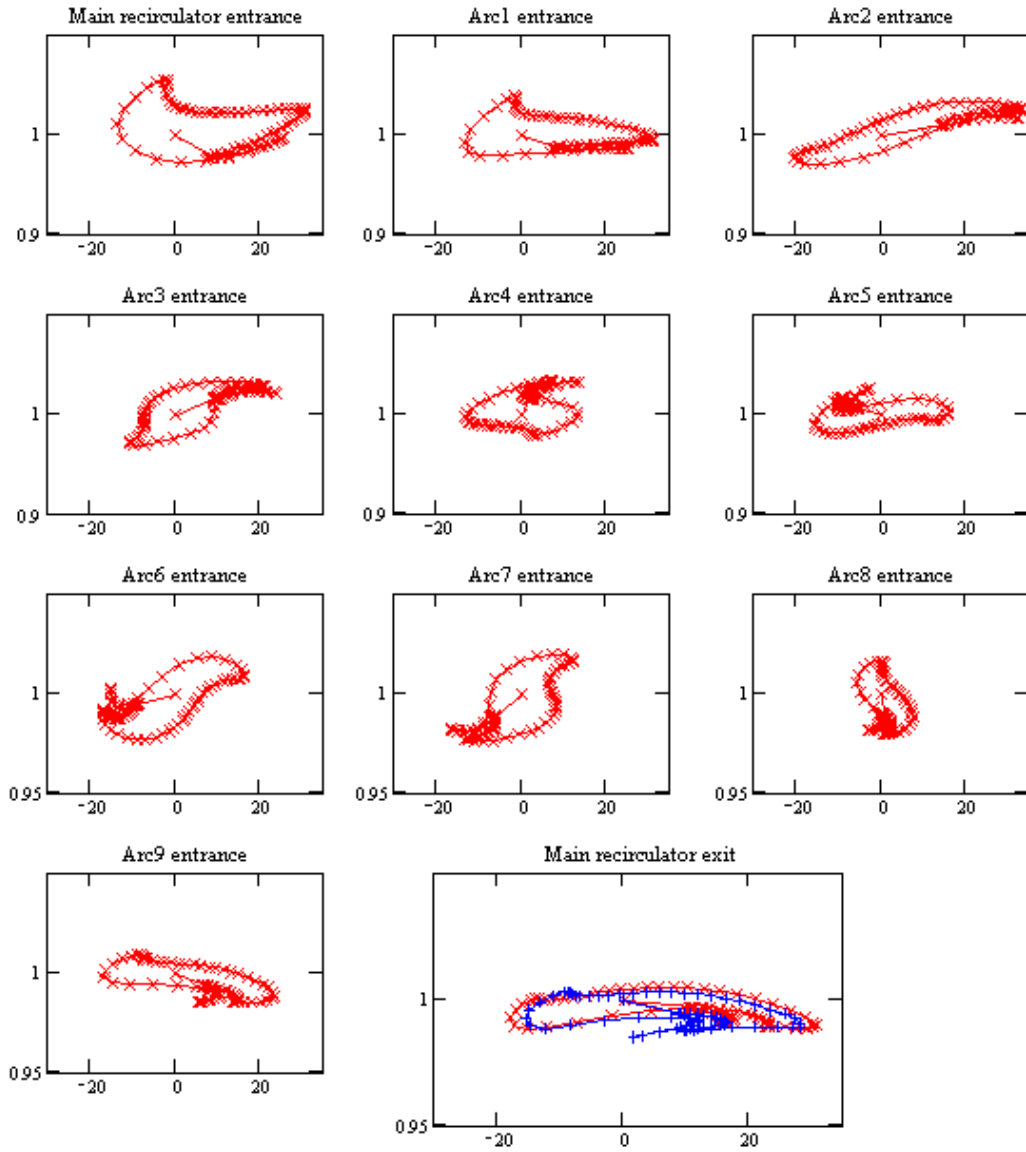


Figure 3: Beam envelopes in the preaccelerator from injection to RLA1 at 2.8 GeV.

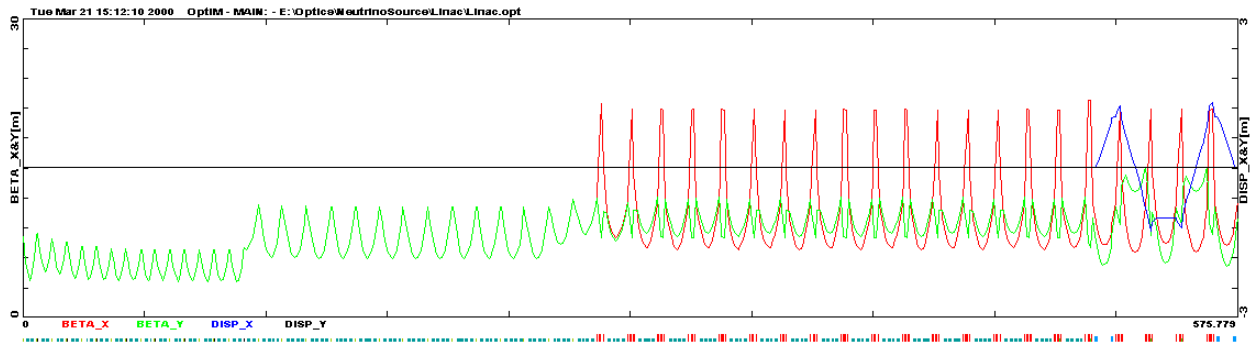


Table 3: Acceleration Parameters

<u>Preaccelerator</u> 200 MHz, 190 MeV/c \rightarrow 2.8 GeV energy; 15 MV/m gradient, accelerating phase $-70^\circ \rightarrow 0^\circ$				
<u>RLA1 (Compressor)</u> 200 MHz, 2.8 GeV \rightarrow 11 GeV energy; 15 MV/m gradient; total voltage/linac: 1.227 GV;				
	Kinetic energy (GeV)	M_{56} (m)	Gang Phase (deg)	Total energy spread $2\Delta p/p$ %
Entrance	2.89		6	11.7
Arc 1	4.11	0.6	-22	9.0
Arc 2	5.25	0.6	-25	9.9
Arc 3	6.36	0.6	-29	9.8
Arc 4	7.43	0.6	-38	9.2
Arc 5	8.40	0.5	-45	9.6
Arc 6	9.26	0.5	-45	9.9
Arc 7	10.13	0.5	-45	9.5
Exit	11.00	0.5		8.2
<u>RLA2 (Primary)</u> 400 MHz, 11 GeV \rightarrow 50 GeV; 15 MV/m gradient; total voltage/linac: 4.25 GV				
	Kinetic energy (GeV)	M_{56} (m)	Gang Phase (deg)	Total energy spread $2\Delta p/p$ %
Entrance	11.00	2.00	-7	8.2
Arc 1	15.22	2.00	-30	6.3
Arc 2	18.9	2.00	-17	6.3
Arc 3	22.96	2.00	-30	6.4
Arc 4	26.64	2.00	-30	5.4
Arc 5	30.32	2.00	-30	4.5
Arc 6	34.00	2.00	-30	4.1
Arc 7	3.68	2.60	-11	4.3
Arc 8	41.85	2.60	-16	3.7
Arc 9	45.94	2.60	-17	2.5
Exit	50.00			1.6

Figure 4: RLA1 – typical RLA1 linac and arc beam envelope functions.

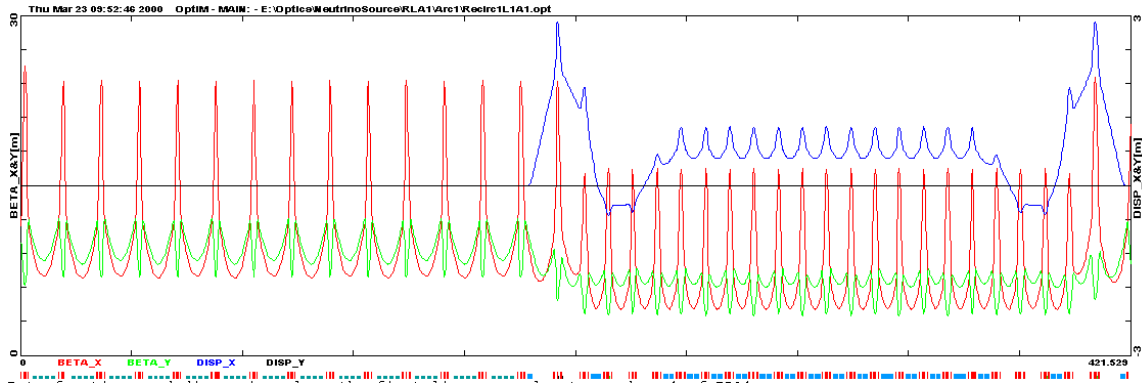


Figure 5: RLA2 – spreader/recombiner geometry

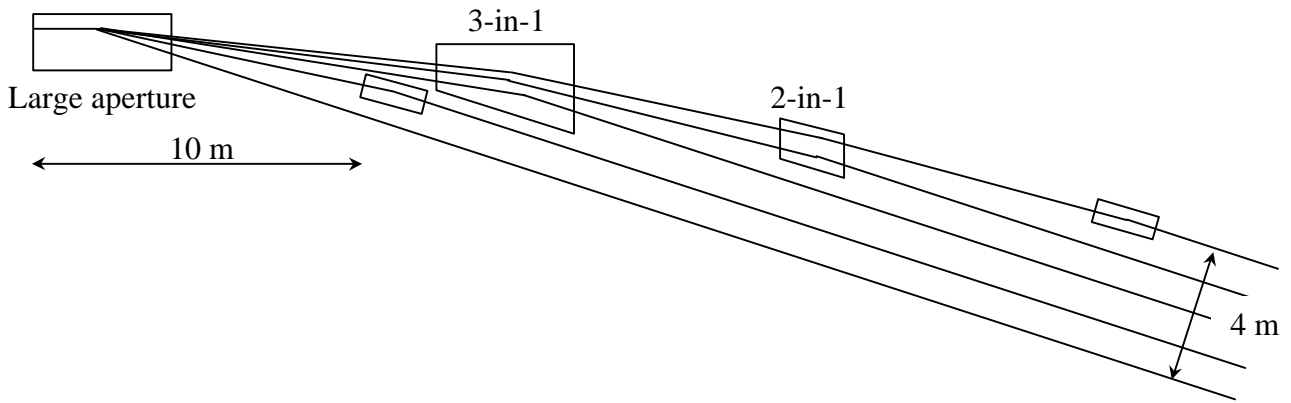
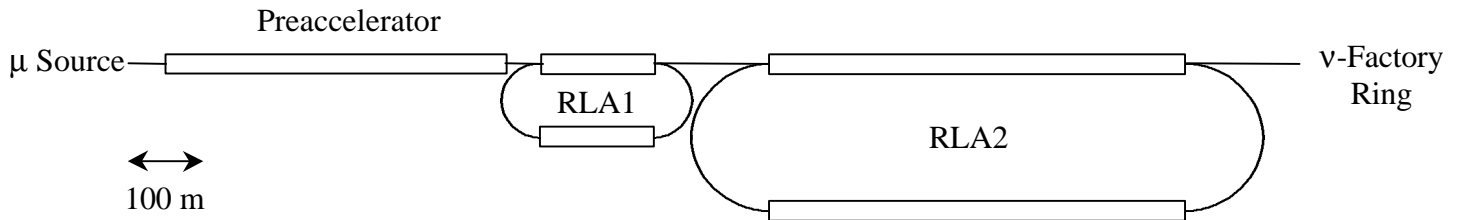


Figure 6: MAD Layout.



Collective Effects – We examine two types of beam breakup (BBU) instabilities relevant to linacs – multipass BBU and cumulative BBU. Multipass beam breakup is of most concern in accelerators in which the beam is passed many times through the same linac structure. The mechanism that causes the instability is the fact that the recirculated beam can be displaced at a given cavity due to a kick it receives from a HOM in the same cavity on a previous pass. The displaced beam can then interact with the fields of the HOM on subsequent passes and feed energy into it causing subsequent bunches to be kicked even harder. There is, therefore, a closed feedback loop between the beam and the HOMs formed within the structure. The M_{12} and M_{34} matrix elements (for the recirculation) are important for the feedback aspect of the instability.

Cumulative beam breakup, on the other hand, results from the beam interacting with two or more cavities that make up the linac. Cumulative BBU begins when a bunch receives a transverse kick from a cavity HOM resulting in a transverse displacement in a downstream cavity. The displaced bunches can drive the HOM at the second cavity coherently thereby transferring kinetic energy into the HOM. Following bunches arriving at the downstream cavity are then more strongly deflected because of the additional energy contained in the HOM.

The important difference between cumulative and multipass beam breakup is that in cumulative beam breakup there is no feedback of the HOM energy of the driven cavity back to the cavity that initially deflects the beam. The cavities act to amplify the beam offsets due to the kick, and this amplification depends strongly on the beam current. The threshold current for cumulative BBU is the current where the offsets are amplified to the point where the beam hits the beam pipe.

CEBAF's multipass BBU threshold current had been calculated to be around 20 mA for external Q's of the HOMs less than 10^5 . Extensive TDBBU simulations seem to indicate that the threshold current scales with the injection and final energies approximately as the square root of the product of the two energies [5]. In addition, the neutrino factory linac will require roughly an order of magnitude more cavities than the CEBAF linac, therefore the impedance will be higher by an order of magnitude. Finally the scaling with the rf operating frequency has been shown to be inversely proportional to the frequency squared, if the accelerating gradient is frequency-independent and inversely proportional to the frequency if the gradient varies linearly with frequency. Assuming the more pessimistic $1/w$ scaling, for $E_{in}=3$ GeV, $E_{fin}=50$ GeV for the neutrino factory and $E_{in}=45$ MeV and $E_{fin}=4$ GeV for CEBAF, we arrive at

$$I_{th} = 20mA \times \frac{1}{10} \times \frac{\sqrt{3GeV \times 50GeV}}{\sqrt{45MeV \times 4GeV}} \times \frac{1500}{200} \approx 433mA.$$

Note that if this was a truly CW linac, the average operating current would be about 50 mA, an order of magnitude lower than the threshold current.

The damping time of the HOMs is $2Q/\omega$ and it is equal to 16 *m*secs for $Q=10^4$ and $\omega = 2\pi f$, where $f \approx 200$ MHz. Therefore during the 10 *m*secs between pulses, the fields have almost “died”, which would imply a somewhat higher threshold for the pulsed machine than for the CW.

Finally, cumulative BBU needs to be examined as it is typical in an S-band linac in the 100 mA range. At 200 MHz the shunt impedance and gradient scaling compounded with the larger apertures should result in a factor of 10-20 higher threshold current. At ~1% duty factor, the equivalent threshold is ~100A.

In conclusion, these rough estimates based on scaling from existing accelerators, would indicate that BBU will probably not be an issue for the neutrino factory linac if external Q 's of HOMs are damped to 10^4 or lower, however detailed simulations must be carried out so that the points outlined here be addressed more rigorously

SRF Technology Issues

The RF implications of a slowly pulsed, recirculated SRF linac with beam macropulse acceleration driven by stored energy can be readily characterized. Recent technology developments suggest we assume the availability of superconducting cavities with the single-cell properties summarized in Table 4.

Here, we assume the availability of 15 MV/m gradients at both 200 and 400 MHz. The assumed Q_0 's are in keeping with those in presently available SRF systems. The stored energy is computed using

$$U_{\text{stored}} = \frac{E^2 I^3}{R/Q} \frac{10^4}{24\pi}$$

with λ the free-space wavelength. These data specify the CW dynamic load from the RF system. It is summarized in Table 5 for CW operation at 4.2° K. The number of cells is simply the installed voltage divided by the single cell voltage in Table 4; the dynamic load is the number of cells times the Table 4 power loss per cell.

Table 4: SRF cavities for MAD: single cell properties

Machine Stage	f (MHz)	l_{cell} (m)	E (MV/m)	V (MV)	$U_{\text{stored}}/\text{cel}$ 1 (J)	Q_0	R/Q (Ω/cell)	P_{lost} (CW, W/cell)
Preaccelerator	200	0.75	15	11.25	1000	6×10^9	100	209
RLA1	200	0.75	15	11.25	1000	6×10^9	100	209
RLA2	400	0.375	15	5.625	125	6×10^9	100	52

Table 5: Dynamic load, 4.2° K operation

Machine Stage	Installed Voltage (GeV)	#cells	CW dynamic load @ 4.2° K (kW)
Preaccelerator	3.6	320	67
RLA1	2.6	231	48
RLA2	8.5	1079	56

The total dynamic CW load is therefore on the order of 171 kW at 4.2° K. We are however of the intent rather to operate the machine in a pulsed mode, filling it prior to injection of the macropulse and accelerating the beam using stored energy. This will significantly reduce the dynamic heat load, by in fact roughly the duty cycle of the RF. In consideration of this operating mode, we present in Table 6 a summary of the energy extraction by the beam macropulse as it traverses each accelerator segment. It presents, in particular, the energy and gradient sag due to the extraction of stored energy by the beam.

Table 6: Energy extraction from single cell during macropulse.

Machine Stage	Charge/macropulse (μC)	# passes	V (MV)	ΔU (J)	$\Delta U/U_{\text{stored}}$ (%)	$\Delta V/V$ Across pulse (%)
Preaccelerator	0.48	1	11.25	5.4	0.5	0.25
RLA1	0.48	4	11.25	21.6	2.2	1.1
RLA2	0.48	5	5.625	13.5	10.8	5.6

We note the relative gradient sag is $\sim 1/2$ that of the stored energy, due of course to the fact the energy scales as the square of the gradient. The gradient sag will impose an energy slew along the macropulse, with the tail of the pulse experiencing less acceleration than the head. Given the large inherent energy spread of the beam, the conjectured sag will not be a problem in the preaccelerator or RLA1, but could become significant in RLA2, where the smaller stored energy at higher frequency is more susceptible to influence by the passage of the macropulse. This may be manageable as a part of the RF manipulations performed during longitudinal matching. For example, the RLA2 arc momentum compactness and path lengths might be adjusted to not only do the required microbunch compression but to also accommodate the energy slew induced across the *macropulse*. That this is possible in principle is illustrated by Figure 2; the final frame in each of 2a and 2b includes data illustrating the beam loading induced energy slew from the head to the tail of the bunch train. The longitudinal match used to manage the large beam phase space similarly controls spread across the macropulse. Once a final design is established, a methodology to operationally implement this process must be developed.

Also critical to this scenario is the availability of ~ 15 MV/m gradient at 400 MHz. Should the gradient be lower, the stored energy will fall and the gradient droop increase significantly, aggravating this effect. This may ultimately motivate the use of 200 MHz

RF in RLA2 with an associated increase in dynamic load but with less risk to machine performance. A detailed design study must evaluate this cost/risk/benefit tradeoff. Given, however, the availability of adequately high gradients and the development of an operationally appropriate longitudinal matching scenario to both compress the microbunch phase space and manage gradient sag across the macropulse, it appears the “slow fill, accelerate, slowly refill” scenario can be applied in this system with adequate performance. Moreover, a contingency use of 200 MHz in all machine stages clearly allows this mode of operation.

Details of pulsed operation evolve from consideration of RF drive power requirements. Table 7 presents power demands for each of the machine stages. The average beam loading current is just the product of the macropulse charge (0.48 μC), the repetition rate (15 Hz) and the number of passes through the segment; the average extracted power is product of the single cell voltage and the average beam loading current. The power to control microphones and detuning is the product ($U_{\text{stored}} \times \delta\omega$) of the stored energy and the detuning bandwidth $\delta\omega$, here taken to be $2\pi \times 80$ Hz. Though an approximation, this result is valid in this parameter regime, where the detuning bandwidth is much greater than the intrinsic. We note that the result is the power required for an infinite filling time, and therefore remark that the information to be drawn from this discussion is not the particular RF power demanded, but rather that the power is, at these low currents, dominated by establishing and maintaining the fields in the presence of detuning. It is therefore important to properly optimize the coupling by setting the loaded Q with some care.

Table 7: Single cell RF power requirements.

Machine Segment	# passes	I_{average} (μA)	V (MV)	P_{average} (W)	$U_{\text{stored/cell}}$ (J)	P_{control} for 80 Hz bandwidth, (kW)
Preaccelerator	1	7.2	11.25	81	1000	503
RLA1	4	28.8	11.25	324	1000	503
RLA2	5	36	5.625	203	125	63

Optimization of Q_L is typically accomplished by selecting a coupling minimizing the required RF power at anticipated operating parameters. In the case of infinite filling time, this is straightforward. The RF power is given in terms of cavity parameters by the following expression, in which $\omega = \omega_0 + d\omega$, ω_0 being the cavity angular frequency and $d\omega$ the angular detuning bandwidth [6].

$$P = \frac{(Q_0/Q_L)^2}{4(Q_0/Q_L - 1)Q_0} \frac{V^2}{(R/Q)} \left\{ \sqrt{1 + Q_L^2 \left(\frac{\omega_0}{\Omega} - \frac{\Omega}{\omega_0} \right)^2} + \frac{(R/Q)Q_L I_{\text{average}}}{V} \right\}^2$$

Other parameters are as specified in Tables 4 through 7. Figure 7 presents this RF power as a function of Q_L for several detuning bandwidths at 200 MHz for preaccelerator parameters (Figure 7a) and 400 MHz for RLA2 parameters (Figure 7b). We note that the RLA1 result will be virtually identical to that of the preaccelerator. This is because, as mentioned before, at these low currents the required RF power is dominated by the power required to establish and control the field in the presence of static and dynamic detuning, not by the low average power drawn by the beam. The optimum Q_L is simply the value providing the minimum required power; this can be either read off the Figure 7 curves or derived analytically by minimizing the above power expression with respect to loaded Q for the desired parameter set.

The preaccelerator (and, by implication, RLA1) system will handle ~ 80 Hz detuning with under 500 kW power provided coupling is chosen such that $Q_L \sim 1.25 \times 10^6$. This RF power is within the limits of present technology and can be delivered to the cell through existing, albeit state of the art, couplers. Similarly, the RLA2 system will manage ~ 80 Hz detuning with ~ 125 kW power when the coupling is chosen so that $Q_L \sim 2.5 \times 10^6$. The power requirements are similar to the “back of the envelope” given above, and should be viewed, again, as not providing a final power value but rather, first, that we are working at the zero current limit, and second, as providing information on the dependence of the power on the detuning.

For finite filling times, the analysis is less transparent. In this case (in the zero current limit applicable to this machine), the power as a function of fill time T , coupling $\beta = Q_0/Q_L - 1$, stored energy U , detuning bandwidth $\delta\omega$ and intrinsic bandwidth $\Delta\omega_0 = \omega_0/Q_0$ is as follows.

$$P = \frac{U \Delta\omega_0}{\left[1 - \exp\left(-\frac{T\Delta\omega_0(\mathbf{b} + 1)}{2}\right)\right]^2} \frac{1}{4\mathbf{b}} \left[(\mathbf{b} + 1)^2 + \left(\frac{2d\mathbf{w}}{\Delta\omega_0}\right)^2 \right]$$

The optimum Q_L (or coupling β) is that which minimizes the required power. This case is not amenable to simple analytic treatment because of the time dependence. Instead, a numerical solution is used to minimize the power as a function of coupling. Figure 8 presents the optimum power, coupling, and detuning as functions of fill time for parameter sets appropriate to this machine. The asymptotic limit is simply that given above; as the fill time decreases to below ~ 10 msec, the required power rises and optimum coupling and bandwidth change.

Figure 7: RF power requirements for 200 and 400 MHz single cells.

Figure 7a: 200 MHz, $Q_0=5 \times 10^9$, $V=11.25$ MV, $R/Q=100 \Omega$, $I_{\text{average}}=7.2 \mu\text{A}$

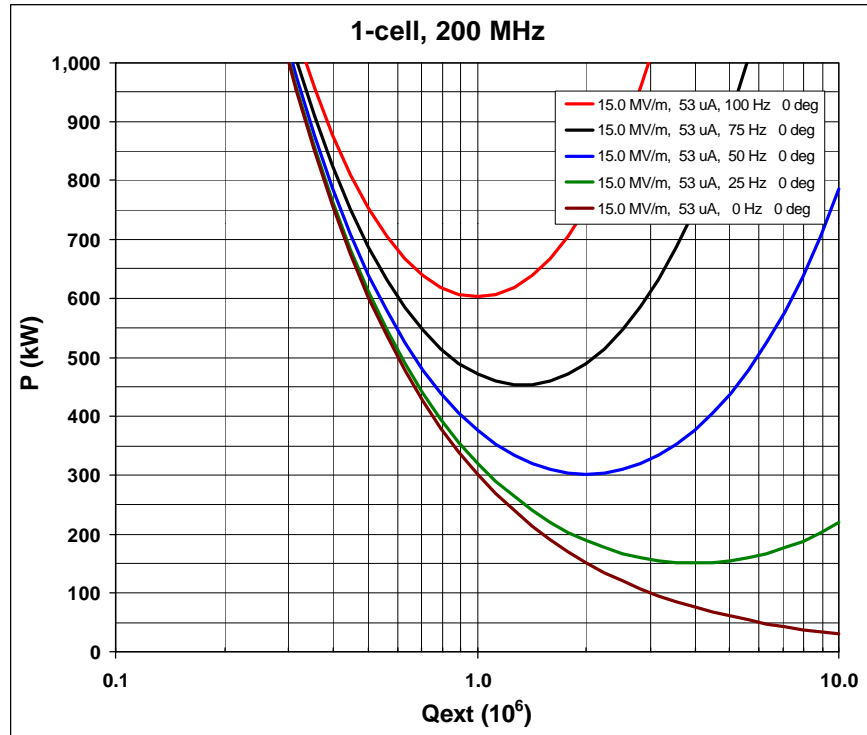


Figure 7b: 400 MHz, $Q_0=5 \times 10^9$, $V=5.625$ MV, $R/Q=100 \Omega$, $I_{\text{average}}=36 \mu\text{A}$

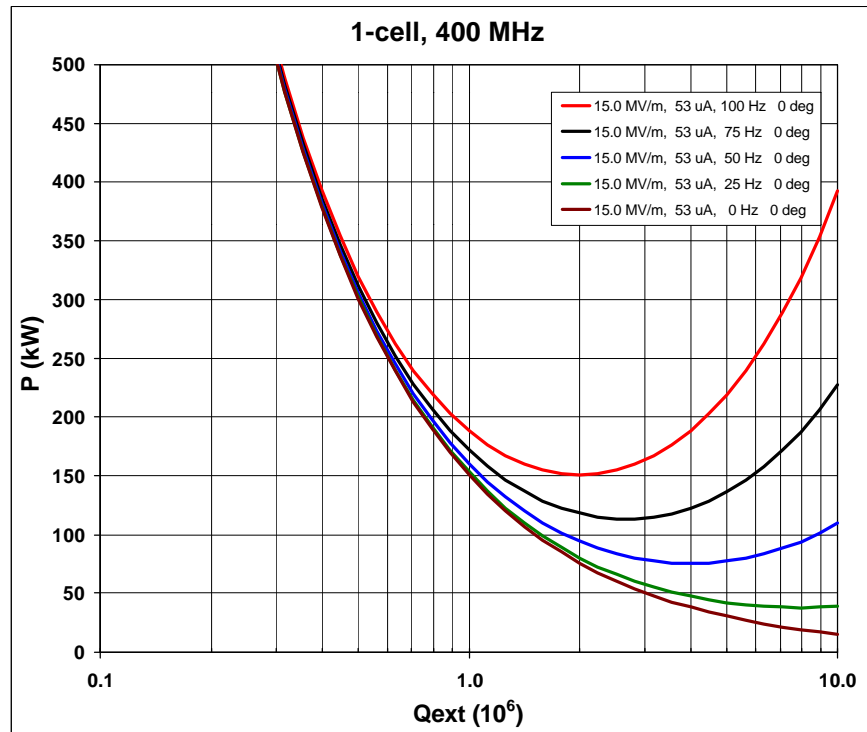


Figure 8: Optimized power, coupling, and bandwidth as a function of fill time.

Figure 8a: 200 MHz system

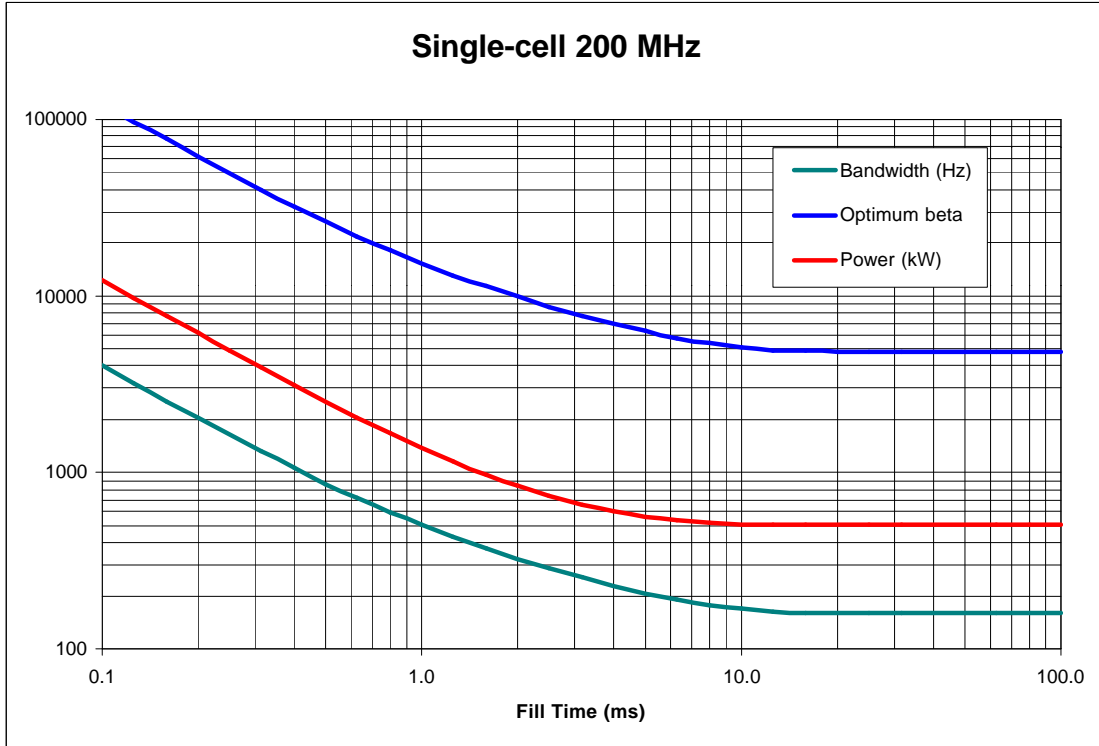
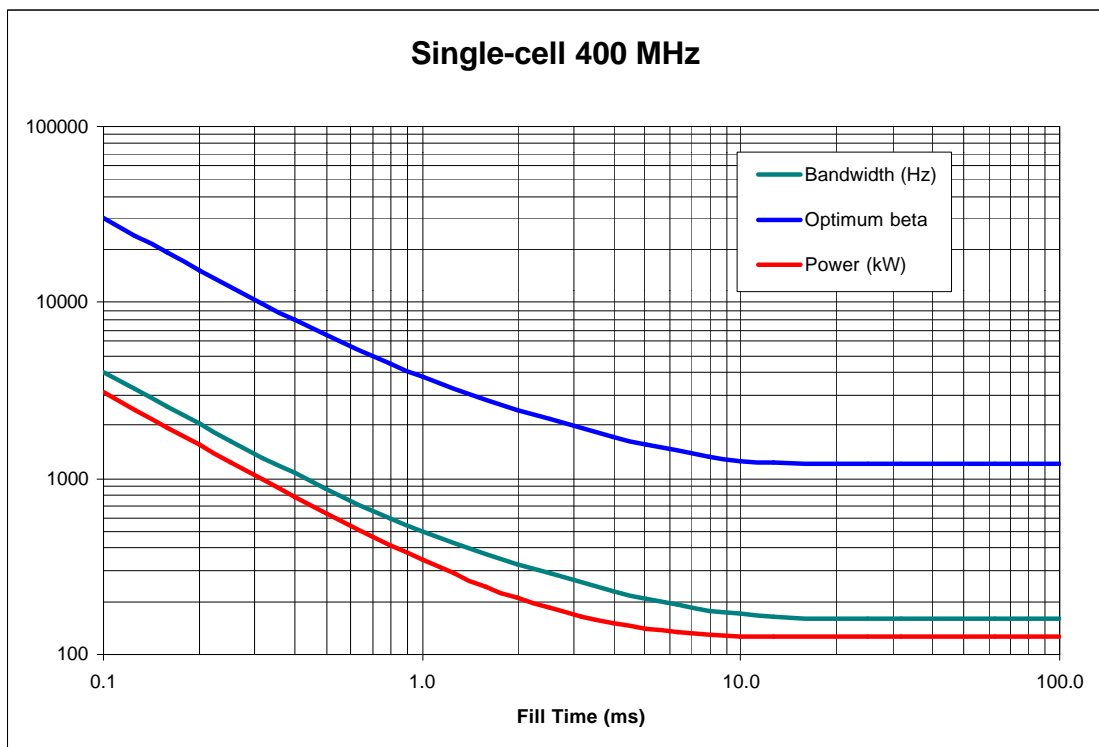


Figure 8b: 400 MHz system



A detailed design must choose a fill time (or duty cycle) consistent not only with RF power requirements, but with the constraint of cryogenic loads in place as well. For this study, we examine a fill time of 4 msec, which corresponds to a duty cycle of 6% at 15 Hz macropulse repetition rate. The preaccelerator and RLA1 will optimally require 600 kW at a coupling of about 7000, corresponding to a Q_L of 8.6×10^5 , while RLA2 will require 150 kW at a coupling of 1800, or a Q_L of 3.3×10^6 . At this duty cycle, the dynamic heat load for the full machine is 6% of the 171 kW CW load quoted following Table 5, or 10 kW. Given the details of a full design, this type of analysis should be executed to establish the cost optimum of the RF drive and cryogenic systems.

Use of modestly long (4 msec) RF pulses and relying on cavity stored energy to accelerate the beam thus allows use of available (though state of the art) couplers, with an associated small dynamic cryogenic load of 10 kW. The required RF power is specified not by the beam but rather by the control system (to manage static and dynamic detuning). The primary issues for this scenario are the availability of sufficiently high gradients (to provide adequate stored energy) and proper specification of the cavity external Q (to optimize RF power and duty cycle/cryogenic requirements).

We note that alternative scenarios are possible. The above discussion details a system in which the beam is accelerated entirely by energy “slowly” stored in SRF cavities between macropulses. Earlier discussions have noted that directly driving the beam with RF power during the macropulse requires prohibitively large peak RF powers (“fast” pulse scenarios). We have not however in this proof-of-principle discussion determined the system-wide optimum linac fill time. It is possible, for example, to reduce beam loading induced momentum spread across the macropulse by adopting an RF fill time that replenishes the stored energy between individual *turns* of the macropulse [7]. Though requiring more peak RF power than refilling between macropulses, this scheme does not require the peak RF power demanded by “fast” pulsing scenarios such as those used in copper linacs, and, in addition, provides better beam momentum spread through the acceleration cycle and allows use of a lower RF duty cycle. It can also reduce the average required RF power. It may therefore provide (through reduced transport and cryogenic demands) lower costs. The detailed system design must address this as an R&D issue by providing a cost/performance optimization amongst peak and average RF power demands, momentum spread driven transport system requirements, and dynamic heat load/cryogenic system loads.

R&D Issues

The preceding cursory design description immediately presents technical issues for resolution. Detailed system beam dynamics and engineering designs must be developed. In addition to providing specifications for areas such as accelerator beam optics, this design must evaluate the viability of the use of 400 MHz RF in RLA2. In particular, it must develop a longitudinal matching scenario which not only manages the single bunch phase space through the acceleration cycle, but in addition compensates the relatively

large gradient sag across the macropulse as it traverses the higher frequency segment of the driver accelerator. A proof of principle is illustrated above, but an operationally applicable implementation should be devised when a detailed design is available. The detailed design should in addition provide a complete quantification of emittance dilution from chromatic effects. It must be the result of a careful cost/performance analysis of the RF drive system (balancing RF pulse length/peak klystron power and average RF power requirements), dynamic heat load (cryogenic system demands being lower for lower RF duty cycle), and the required transport system acceptance (greater acceptance being required as a consequence of greater beam loading across the macropulse).

Two areas present themselves as sources of potential longer-term R&D topics. The first is that of cavity and RF drive development, for which the performance goals of 15 MV/m gradient and $Q \sim 5 \times 10^9$ at 200-400 MHz may require some advancement of presently available technology. Potential rapid dissipation of the large stored energy in such low frequency/high gradient cavities will require some thought on quench protection issues. Control of microphonics in large SRF structures may require effort beyond presently implemented methods.

The second area of development will be related to the driver magnetic systems. Magnetic shielding, particularly in the preaccelerator, will be an issue, inasmuch as high magnetic fields (from focusing solenoids) will be in close proximity to SRF components. A second magnet-related issue will be due to the inevitable loss of muons throughout the system. This will result in relatively high ambient radiation fields and will necessitate study of the effect of radiation on accelerator components, particularly on the superconducting dipoles and quadrupoles proposed for use in the recirculator.

Acknowledgments

Many individuals have contributed materially to this design. Amongst them are:

- our Fermilab contacts, N. Holtkamp, D. Finley, C. Bohn, and D. Neuffer,
- S. Berg of BNL,
- members of the Jefferson Lab Beam Physics and Instrumentation Department,
- “coffee-pot” co-designers J. Benesch, J. Preble, and M. Tiefenback, and G. Neil, and
- Jefferson Lab staff members who participated in a October 1999 design study kick-off meeting, including (in addition to the authors and some previously named co-conspirators) S. Benson, C. Hovater, A. Hutton, L. Merminga, C. Reece and C. Rode.

In addition, L. Merminga graciously performed and documented BBU estimates for the recirculating linacs. The authors thank all who participated for their contributions and apologize to any whose name may have been inadvertently omitted.

Notes and References

- [1] Source parameters were provided by C. Bohn in a 27 September 1999 e-mail.
- [2] For a discussion of linac dynamic range (injected to final energy ratio) see, *e.g.* D. Douglas, “Lattice Design Principles for a Recirculated, High Energy, SRF Electron Accelerator”, Proc. 1993 IEEE Part. Accel. Conf., Washington, DC, May 1993.
- [3] Longitudinal matching scenarios for linacs have been discussed for some time; see, *e.g.*, Geoffrey Krafft, “Non-isochronous Recirculation at CEBAF”, CEBAF-TN-92-005, 23 January 1992. Various analogous solutions for this system were independently developed by D. Neuffer, S. Berg, and V. Lebedev; the latter is presented here and is documented on the Web at <http://www.jlab.org/~lebedev>.
- [4] V. Lebedev, *op. cit.*
- [5] J. J. Bisognano, private communication.
- [6] G. A. Krafft, S. N. Simrock, and K. L. Mahoney, “Beam Loading Studies at CEBAF”, in the Proc. of the 1990 Linear Accelerator Conference, September 1990, Santa Fe. LANL Report LA-12004-C.
- [7] G. A. Krafft, JLAB-TN in preparation.